Clinical Complementary Medicine and Pharmacology 2 (2022) 100010

Contents lists available at ScienceDirect

Clinical Complementary Medicine and Pharmacology

journal homepage: www.elsevier.com/locate/ccmp

Shen-Qi-Wan Protects the Renal Peritubular Capillary Injury from Adenine-mediated Damage by Upregulating Aquaporin 1

Yuting Bao[a,1], Yehui Zhang[a,1], Yuanxiao Yang[b], Xueming Chen[a], Luning Lin[a], Yunbo Fu[a], Liting Ji[a,*], Changyu Li[a,*]

[a] School of Pharmaceutical Sciences, Zhejiang Chinese Medical University, 548 Binwen Road, Hangzhou 310053, Zhejiang, China
[b] School of Basic Medical Sciences and Forensic Medicine, Hangzhou Medical College, Hangzhou 310053, Zhejiang, China

ARTICLE INFO

Keywords:
Chronic kidney disease
Peritubular capillary injury
Shen-Qi-Wan
AQP1
VEGF
Adenine

ABSTRACT

Background: Shen-Qi-Wan (SQW), a commonly used prescription against chronic kidney disease (CKD) in Traditional Chinese Medicine (TCM), has a nephroprotective action in adenine-induced kidney injury. However, the mechanism of SQW in renal injury remains unclear.

Objective: This study was undertaken to measure the effect of SQW on peritubular capillary injury both *in vivo and in vitro* assays.

Methods: The effect of SQW on the peritubular capillary injury was evaluated according to measuring hypothalamic-pituitary-adrenal (HPA) function, inflammatory cytokines, VEGF (vascular endothelial growth factor), CD34 (Cluster of differentiation 34), and AQP1 (Aquaporin 1) levels in the kidney, cell migration, and lumen forming capacity.

Results: SQW supplementation could ameliorate dysfunction of the HPA and renal function loss induced by adenine. SQW also significantly inhibited the inflammatory cytokines including MCP-1 (monocyte chemotactic protein-1) and VCAM-1 (vascular cell adhesion molecule-1) level. Alternatively, SQW administration showed an ameliorating effect from the toxicity and alleviated the injury of capillaries around renal tubules instigated by adenine through increasing AQP1 mRNA and protein level. SQW medicated the serum enhanced the migration and lumen formation ability of HMEC-1 cells, and significantly increased AQP1 protein level. Moreover, AQP1 knockdown efficiently inhibited the migration and lumen formation ability in HMEC-1 cells, and weakened the effect of SQW medicated serum.

Conclusion: These results suggested that SQW attenuated peritubular capillary injury in adenine-induced CKD model rats through boosting angiogenesis in endothelial cell, and AQP1 may be a potential target of SQW for treating the renal injury.

1. Introduction

Chronic kidney disease (CKD), also called chronic kidney failure, was the gradual loss of kidney function due to different anamolies like-types- 1 or 2 diabetes, high blood pressure, glomerulonephritis, interstitial nephritis, polycystic kidney disease (Romagnani et al., 2017). It is considered a severe public health problem, leading to death due to failure in the cardiovascular and renal systems (Wuttke et al., 2019). It has been estimated that about 10% of the world's population was afflicted with CKD (Qiu et al., 2018). Therefore, the prevention and therapeutic measures for CKD in a preclinical system have to be addressed, aggressively.

The pathological syndrome of CKD was renal function loss, including glomerular sclerosis (Lemley, 2016; Munoz-Felix et al., 2014), tubular atrophy (Denic et al., 2016), and interstitial fibrosis (Li et al., 2019; Roediger et al., 2018). Studies showed that peritubular capillary rarefaction prominently correlates with impaired kidney function. Moreover, peritubular capillary rarefaction is a prominent histological characteristic of CKD and a central driving force of CKD progression (Babickova et al., 2017). Studying the pathophysiological changes of capillary endothelial cells, protecting the capillaries of the kidney, and improving renal microcirculation have received more and more attention in the treatment of CKD (Rabelink et al., 2007; Venkatachalam et al., 2015). Capillary endothelial cells can instantly switch to an activated migratory state in response to growth factor stimuli, primarily through vascular endothelial growth factor (VEGF) signaling (Eelen et al., 2018). Therefore, the present study considered examining the pivotal regulator of CKD progression, such as peritubular capillary rarefaction.

* Corresponding authors.
E-mail addresses: jltzcmu@sina.com (L. Ji), lcyzcmu@sina.com (C. Li).
[1] These authors contributed equally to this work.

https://doi.org/10.1016/j.ccmp.2021.100010
Received 27 April 2021; Received in revised form 8 November 2021; Accepted 13 November 2021

Traditional Chinese medicines have plenty of beneficiary properties, but insufficient evidence prevents them from being mainstream orthodox medicine. Shen Qi Wan (also known as Gui Fu Di Huang Wan; SQW) is a famous Chinese alternative medicine, widely used against kidney disorders (Wang et al., 2016). The components of SQW are composed of eight traditional Chinese herbs-Dihuang, Danpi, Shan Zhuyu, Fulin, Shanyao, Zhexie, Rougui, and Fuzi (Table 1). In a recent study, SQW treatment alleviated renal morphological changes and reduced inflammatory activity, glomerular necrosis in adenine-induced CKD model rats (Chen et al., 2017). Studies demonstrated that components of SQW are also closely associated with the angiogenesis process. Diosgenin (extracted from the root of wild yam) treatment enhanced endothelial proliferation and angiogenesis activating via HIF-1α and VEGF pathways to boost bone formation and the process of fracture healing (Yen et al., 2005). Catalpol, an active component of Radix Rehmanniae, used in the treatment of neurodegenerative diseases, ischemic stroke, metabolic disorders has been experimentally demonstrated that it can improve angiogenesis in rats' stroke model (Dong et al., 2016).

Aquaporin (AQPs) membrane receptors are extremely abundant in the nephron. AQPs act as membrane water channels that involve the secretion and absorption of water and also maintain the osmotic balance of the cell membrane (Verkman et al., 2014). The majority of AQP1 is distributed in the proximal and basement membrane cells of the kidney's proximal tubules, the descending branch of medullary stenosis, and the small vascular endothelial cells (van Koppen et al., 2012). Increasing evidence disclosed that AQP1 involves microvessel formation and cell migration (Palethorpe et al., 2018; Zhou et al., 2019). Thus, AQP1 might be closely related to peritubular capillary rarefaction. Based on the above research background, we hypothesized that SQW treatment might alleviate peritubular capillary rarefaction through enhancing AQP1 expression in the kidney. We examined the beneficiary effect of SQW on the adenine-induced CKD model system and explored whether SQW could improve the perivascular circumference in AQP1 knockdown-HMEC-1 cell.

2. Materials and Methods

2.1. Drugs

SQW (Batch No. 16,1101), Chinese patent medicine, was purchased from Henan Wanxi Pharmaceutical Co., Ltd.(Henan, China). The quality control of SQW of different batch numbers measured by high-performance liquid chromatography (HPLC) analysis met the requirements of the 2015 version of Chinese pharmacopoeia. The total average quantity of Morroniside and logan was 6.46 mg/g, and paeonol was 4.3 mg/g (Zheng, 2018). The main five components (higenamine, coryneine chloride, salsolinol, o-anisaldehyde, and cinnamic acid) belonging to the *jun* herbs *Ramulus Cinnamomi* and *Radix aconiti lateralis preparata* were detected by ultra-performance liquid chromatography (UPLC) (Zhang et al., 2019).

2.2. Animals

Male SD rats in SPF grade (n = 30; age 8 weeks; weight 250 ± 10 g) were purchased from Shanghai Xipuer Bikai Experimental Animal Co. Ltd. (Laboratory animal production license number: SCXK (Shanghai) 2013–0016). Rats were housed in an environmentally controlled barrier room of Animal Center of Zhejiang University of Traditional Chinese Medicine with optimal ambient temperature (20 ± 2 °C) and humidity of 50–60%. Sterilized food and water were provided. The Laboratory breeding room license number was SYXK (Zhejiang) 2013–0184.

All 30 rats were randomly divided into control group, and model group (adenine-induced CKD), and three doses of SQW treatment group (1.5, 3, and 6 g/kg/d, n = 6 in each sub-group). The dosage of adenine was 150 mg/kg BW/day. The model group and three doses of SQW groups were administrated with adenine for 2 weeks. In the next 3 weeks, three doses of SQW groups were continuously administered with adenine supplemented with SQW, while the model group was supplemented with water. The volume of gavage was 0.1 ml/10 g BW.

According to the conversion method of the dosage of experimental animals and humans, the dosage of 3.0 g/kg BW SQW is equivalent to 3.7 times the clinical dosage.

2.3. Ethics statement

The animal experiment was approved by the Ethics of Committee of Zhejiang Traditional Chinese Medical University (Ethical review resolution number: ZSLL-2017-054). All experimental procedures were performed under the Provision and General Recommendation of the Chinese Experimental Animal Administration Legislation. All rats were anesthetized by intraperitoneal injection of sodium pentobarbital at a dose of 50 mg/kg, euthanized by carbon dioxide. All efforts were made to minimize animals suffering.

2.4. H & E Staining

The kidney tissues from each group were fixed in 10% formaldehyde. After paraffin embedding, the tissues were sectioned into 3–5 μm thickness for H & E staining. The pathological conditions of renal tissues from different groups were observed under a light microscope (Leica, Germany). The results of H&E staining were observed for the morphology and structure of the rat's kidney tissues.

2.5. ELISA

The hypothalamus, serum, and urine samples were collected. 9 vol. of PBS (Solarbio, Beijing, China) were added with the isolated hypothalamus and centrifuged at 2000 rpm for 10 min. Collected blood samples were centrifuged at 3000 rpm for 10 min. The urine was collected and centrifuged at 3000 rpm for 5 min. The levels of ACTH, CORT, VCAM-1, VEGF, and U-TP were measured according to the manufacturer's instructions in the ELISA kit (Shanghai Xinfan Biotechnology, Shanghai, China). The automatic biochemical detector is used to detect the content of blood urea nitrogen (BUN), serum creatinine (Scr) and urinary 17-hydroxy corticosteroid (17-OHCS).

2.6. Immunohistochemistry

Parrafin-embedded renal sections (3–5 μm) were baked in an incubator at 60 °C for 2 h and then washed in distilled water for 2 min. The tissue sections were quenched using 3% H_2O_2 for 10 min followed by washing in PBS. Tissue sections were incubated with anti-Aquaporin 1 primary antibody (Abcam, Cambridge, UK), anti-CD34 primary antibody (HUABIO, Hangzhou, China), and anti-VEGF primary antibody (HUABIO, China) at 37 °C for 60 min. After washing with PBS, tissue sections were incubated with secondary antibodies (LI-COR, USA) at 37 °C for 60 min. The DAB substrate system was used to develop the color. The images were captured in a bright field digital microscope, and the analysis was performed by open source Image J software (NIH, USA).

2.7. qPCR

Total RNA was extracted from the tissues using the MiniBEST Universal RNA Extraction kit (Takara, Japan). The cDNA was prepared using RNA reverse transcription kit PrimeScript^{TM} RT reagent (Takara, Japan). And The gene expression was analyzed using qPCR kit SYBR Premix Ex Taq II (Takara, Japan). The relative quantitative analysis of gene expression was complied with the $2^{-\Delta\Delta ct}$ method. All specific primer sequences used in experiments are listed in Table 2.

Table 1
Formulation of Shen-Qi-Wan.

Chinese names	Pharmacognostic nomenclature	Botanical nomenclature	Proportion of ingredients (100%)
Dihuang	Rehmanniae Radix Praeparata	*Rehmannia glutinosa* Libosch.	29.7
Danpi	Moutan Cortex	*Paeonia suffruticosa* Andr.	11.1
Shan Zhuyu	Corni Fructus	*Cornus officinalis* Sieb. et Zucc.	14.8
Fulin	Poria	*Poria cocos* (Schw.) Wolf	11.1
Shanyao	Dioscoreae Rhizoma	*Dioscorea opposita* Thunb.	14.8
Zhexie	Alismatis Rhizoma	*Alisma orientalis* (Sam.) Juzep.	11.1
Rougui	Cinnamomi Cortex	*Cinnamomum cassia* Presl	3.7
Fuzi	Aconiti Lateralis Radix Praeparata	*Aconitum carmichaelii* Debx.	3.7

Table 2
List of specific primer sequences.

Sl.no	Gene	Primer	Rat sequence 5'-3'	Human sequence 5'-3'
1	AQP1	AQP1-F	CTGGATGTGGTTGCTGTGGT	CCGCAATGACCTGGCTGATGG
		AQP1-R	CCTCCATGTAGCAGGCATTG	CGCCTCCGGTCGGTAGTAGC
2	β-actin	β-actin-F	GCTCTCTTCCAGCCTTCCTT	GGGACCTGACTGACTACCTC
		β-actin-R	GGTCTTTACGGATGTCAACG	TCATACTCCTGCTTGCTGAT

2.8. Western blot

Total protein was extracted from the renal tissue in RIPA lysis buffer (Beyotime, China) mixed with 1% phosphatase inhibitor (CWBIO, China), 1% protease inhibitor (CWBIO, China), and 1% PMSF (Beyotime, China). The protein concentration was estimated by the BCA method. The protein was separated using SDS-PAGE gel and transferred onto a PVDF membrane (162–0177, BIO-RAD, USA). The membranes were blocked in 5% skimmed milk (BD, America) in PBST for 90 min, and later, incubated with primary antibodies (anti-Aquaporin 1(Abcam, UK), anti-CD34(HUABIO, China), anti-VEGF(HUABIO, China), anti-β-actin(HUABIO, China)) overnight at 4 ˚C. Later, the primary antibody labeled membranes were incubated with specific secondary antibodies. The protein expression was visualized through Odyssey two-color infrared laser imaging system (Odyssey Clx, USA), and was analyzed with the following formula: $Relative\ gray\ value = (\frac{sample\ gray\ value/sample\ internal\ parameter}{control\ gray\ value\ /\ control\ internal\ parameter})$

2.9. SQW containing serum isolation and purification

Twenty SPF male SD rats were marked, weighed, and randomly divided into the normal control and SQW (3.0 $g{\cdot}kg^{-1}$) groups, with 10 rats in each group. The rats in the SQW group were given a gavage of 100 g/1 mL by intragastric administration twice a day for 5 consecutive days. The normal control group received the same volume of saline. During the administration period, the rats were on a regular diet. However, they were not provided with food, but water was allowed 12 h before the last administration.

After the last dose of SQW administration, rats were anesthetized, and cardiac blood was collected under aseptic conditions. It was allowed to stand for 1 h after isolation and centrifuged at 3000 rpm for 15 min. The collected serum was sterilized by filtration 0.22 μm filter (Millipore, USA). The sterilized serum was then heat-inactivated at 56 ˚C for 30 min in a water bath.

2.10. Cell culture

HMEC-1 cells (iCell Bioscience, China) were grown in Endothelial Cell Medium (ECM) containing 10% fetal bovine serum (FBS), 10 $ng{\cdot}mL^{-1}$ Epidermal Growth Factor (EGF), 1 $\mu g{\cdot}mL^{-1}$ hydrocortisone acetate, 10 mM glutamine, 1% penicillin and streptomycin (1:1). The cells were maintained in an incubator with 5% carbon dioxide (Thermo, USA) at 37 ˚C. The cells were administrated with different doses of serum containing SQW and normal serum. The specific groups included 10% of normal rat serum group (10% NRS), 5% each of SQW-normal rat serum mix group (5% SQW + 5% NRS), and different concentrations of SQW-containing serum diluted with normal rat serum. The cells were starved for 2 h in a serum-free medium before the treatment.

2.11. AQP1 RNAi Lentivirus transduction

HMEC-1 cells (2×10^5) were seeded in a 6 well plate, incubated for 24 h, and transduced with RNAi-expressing lentivirus particles. The RNAi-AQP1 lentivirus (V1 and V2) and negative control lentivirus (NC) were purchased from Genechem Co., LTD (Shanghai, China). AQP1 transfection efficiency was observed after three days from the transduction by qRT-PCR and Western Blot.

2.12. Cell scratch assay (migration assay)

3×10^5 HMEC-1 cell was seeded in a 6 well plate. Before the treatment, the cells were washed with PBS (Solarbio, China), and each group was added with corresponding drug-containing serum and photographed at 0, 6, 12, 24 h. Analysis of the migration area was determined by LAS V4.4 software.

2.13. In vitro *lumen formation assay*

Matrigel gel (60 μL/well) was added to the 96 well plate and placed in an incubator for 30 min to solidify. The HMEC-1 cell suspension was prepared and added to the 96 well plate containing Matrigel gel. Different types of serum were added. After culturing in the incubator for 4 h at 37 ˚C, random fields were selected and photographed. The image was processed by Image *J* software.

2.14. Statistical analysis

The SPSS19.0 statistical software was used to perform a normality test on data set, which was confirmed to the normal distribution, using One-Way ANOVA. If the equation is homogeneous, the LSD test was used. Otherwise Games-Howell (A) test was employed; $P < 0.05$ and $P < 0.01$ were considered statistically significant.

3. Results

3.1. Effect of SQW on renal morphological

The renal injury was induced by adenine treatment in the rat. As shown in Fig. 1A, the structure and morphology of glomeruli and re-

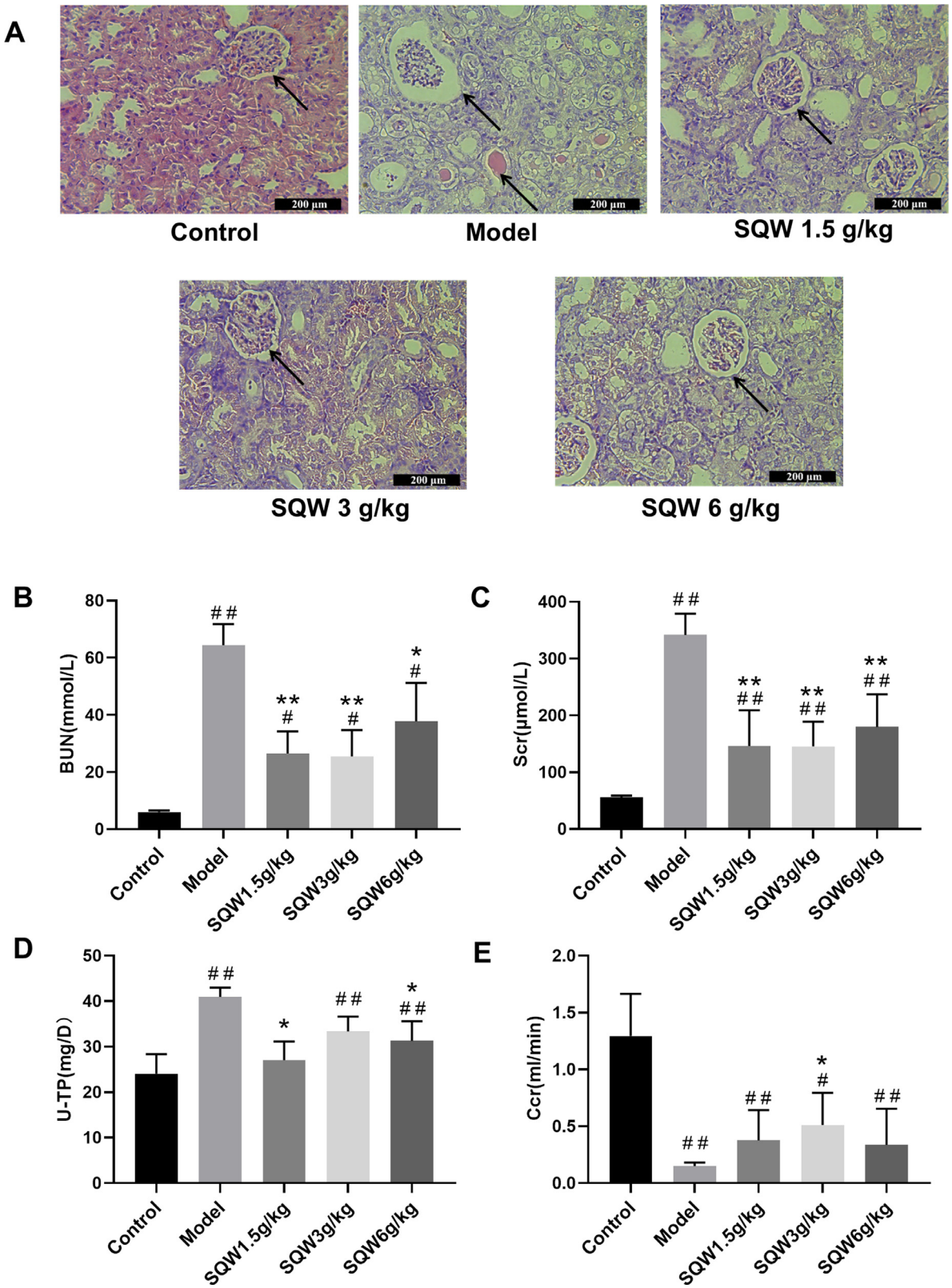

Fig. 1. The effect of SQW on kidney injury in rats. (A) Respective images of HE stained kidney tissue. (B–E) Indices for renal function, including levels of blood urea nitrogen (BUN), serum creatinine (Scr), 24 h urine protein excretion (U-TP) and creatinine clearance (Ccr) in rats (n = 6). Small horizontal bars indicate the mean ± S.D. $^{\#}$ $P < 0.05$, $^{\#\#}$ $P < 0.01$ compared with control group; * $P < 0.05$, ** $P < 0.01$ compared with model group. (Control (Saline), animal model (Adenine-induced chronic kidney disease) and SQW treatment (1.5 g/kg, 3 g/kg and 6 g/kg) in the model animal.)

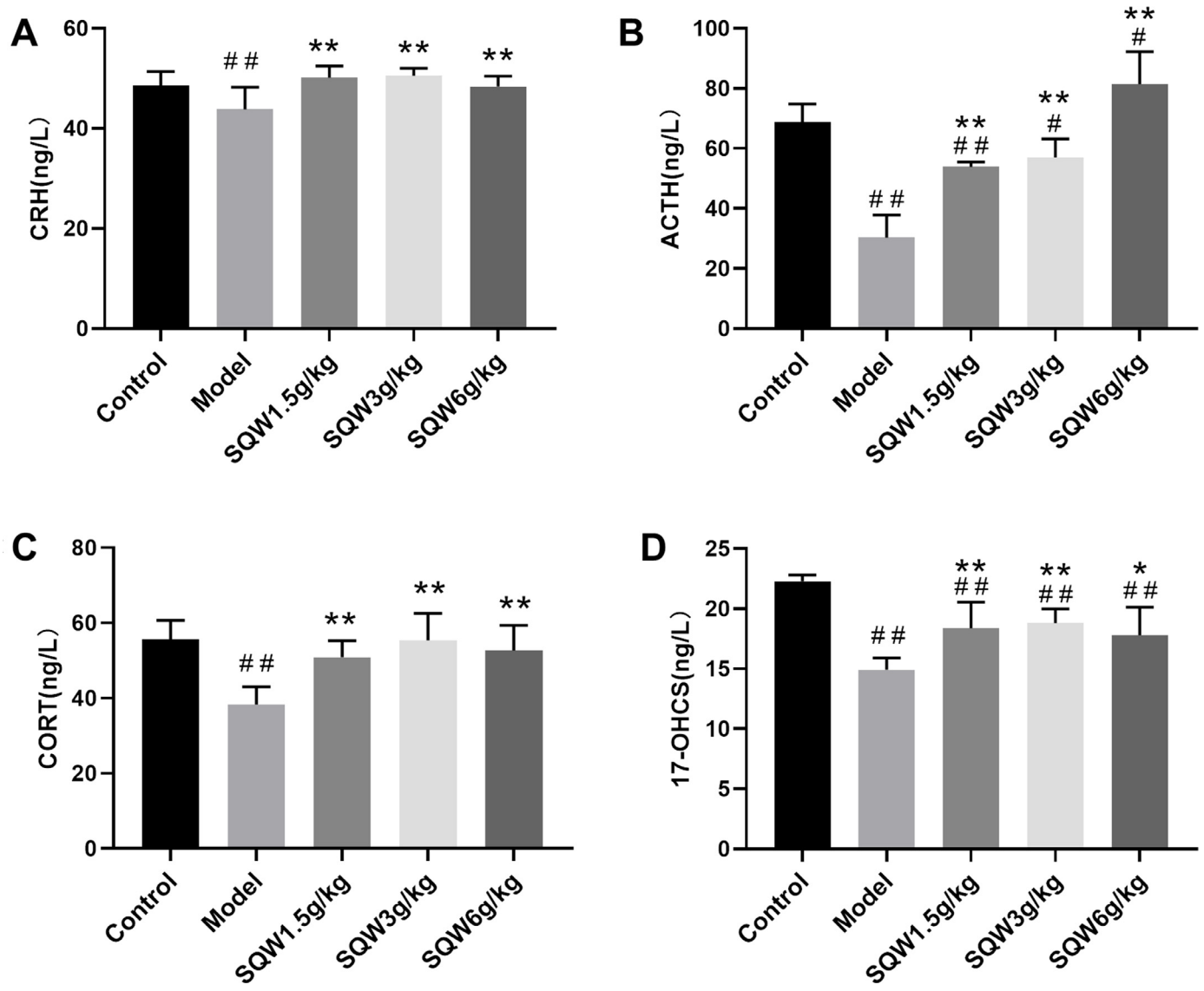

Fig. 2. The effect of SQW on CRH, ACTH, CORT and 17-OHCS in rats. (A–D) Indices for well-established CKD model rats, including levels of hypothalamic CRH, serum ACTH, CORT and urine 17-OHCS in rats ($n = 6$). Small horizontal bars indicate the mean ± S.D. $^{\#}$ $P < 0.05$, $^{\#\#}$ $P < 0.01$ compared with control group; * $P < 0.05$, ** $P < 0.01$ compared with model group.

nal tubules were deformed and damaged. More specifically, histological examination revealed that in the adenine treated (model) group, the glomerulus internal structures collapsed, the renal tubules dilated, the lumens deposited, and the renal tubules blocked as compared with control groups. The administration of different doses of SQW alleviated the adenine-mediated structural damages.

3.2. Biochemical analysis of renal toxicity

In Fig. 1B–E, the levels of BUN ($P < 0.01$), Scr ($P < 0.01$) and U-TP ($P < 0.01$) were significantly elevated in the model group as compared with the normal control groups and in contrast, Ccr ($P < 0.01$) level was decreased in the model group as compared with the normal control group. The corresponding indicators' changes in the SQW group pointed out the beneficial nature of the drug in reducing renal toxicity.

3.3. HPA axis functioning analysis

Adenine treatment in the rat observed in Fig. 2 A–D was toxic as the CRH ($P < 0.01$), ACTH ($P < 0.01$), CORT ($P < 0.01$), and 17-OHCS ($P < 0.01$) levels were diminished compared with normal control rats. Moreover, treatment with SQW elevated the enzyme levels in rats.

3.4. Recovery of VEGF expression by SQW in renal tissues

To examine the effect of SQW on alleviating perivascular capillary damage induced by adenine in rats, the anti-VEGF antibodies in rat kidney sections were employed (Lin et al., 2011). As shown in Fig. 3.A, the VEGF expression was mainly observed on the cell membrane and cytoplasm regions. Adenine led to a reduction in VEGF expression as compared with normal control groups. On the other hand, SQW (3 $g{\cdot}kg^{-1}$) enhanced VEGF expression compared with the model group.

3.5. Recovery of perivascular capillary density by SQW in renal tissue

Perivascular capillary density was labeled by anti-CD34 antibody staining. The CD34 staining was reduced in the model group of rats compared with the control group. As shown in Fig. 3B, the dose of 3 $g{\cdot}kg^{-1}$ SQW was most effective against adenine toxicity.

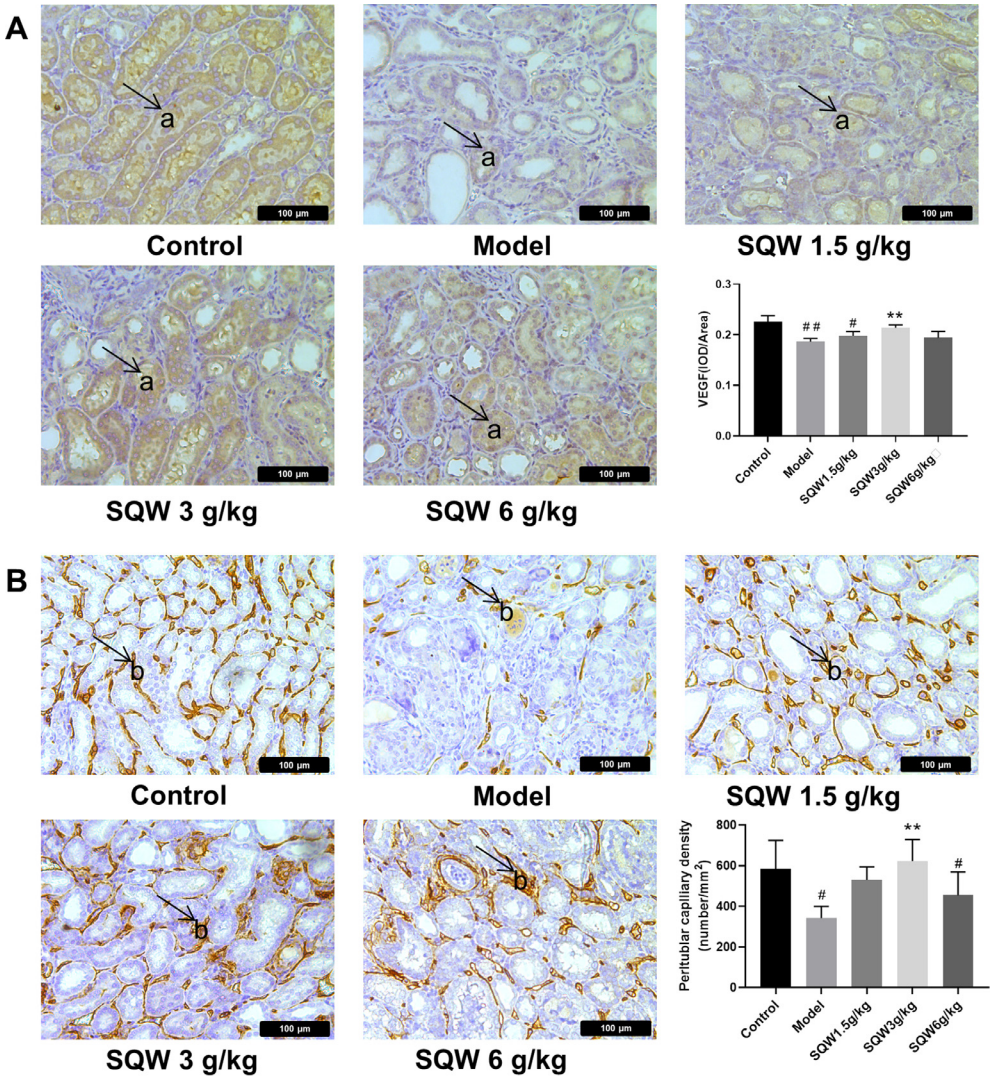

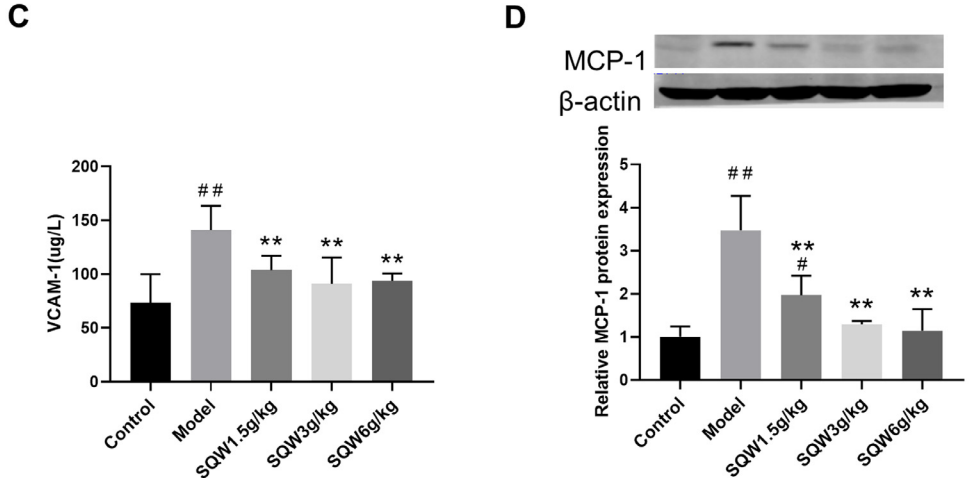

Fig. 3. The effect of SQW on capillary endothelium of renal tubule in rats. (A) Indice for perivascular capillary damage- Immunohistochemistry was used to assess the VEGF in kidney tissue of rats (n = 3). (a) Brown granules represent positive expression of VEGF protein. (B) Indice for perivascular capillary injury- Immunohistochemistry of CD34 protein in the kidney of rats. CD34 protein is localized in the cell membrane (n = 3). (b) Brown or tan granules represent positive CD34 protein. (C) Indice for inflammation followed by perivascular capillary injury-The serum level of pro-inflammatory cytokine vascular cell adhesion molecule-1 (VCAM-1) in rats (n = 6). (D) Indice for inflammation followed by perivascular capillary injury-Western blot of monocyte chemotactic protein-1 (MCP-1) in kidney tissue of rats (n = 6). Small horizontal bars indicate the mean ± S.D. $^{\#}$ $P < 0.05$, $^{\#\#}$ $P < 0.01$ compared with control group; * $P < 0.05$, ** $P < 0.01$ compared with model group. (For interpretation of the references to color in this figure legend, the reader is referred to the web version of this article.)

3.6. Ameliorating inflammatory cytokines by SQW in renal tissue

The Fig. 3C, D dipicts VCAM-1 ($P < 0.01$), and MCP-1 ($P < 0.01$) expression which was increased in the model group compared with the normal control group. VCAM-1 and MCP-1 expressions were reduced in SQW groups versus model group (Fig. 3C, D).

3.7. Effect of SQW on AQP1 in the kidney

As shown in Fig. 4, adenine treatment significantly suppressed the AQP1 expression in both mRNA and protein levels. Moreover, the SQW supplement eventually enhanced the AQP1 expression level.

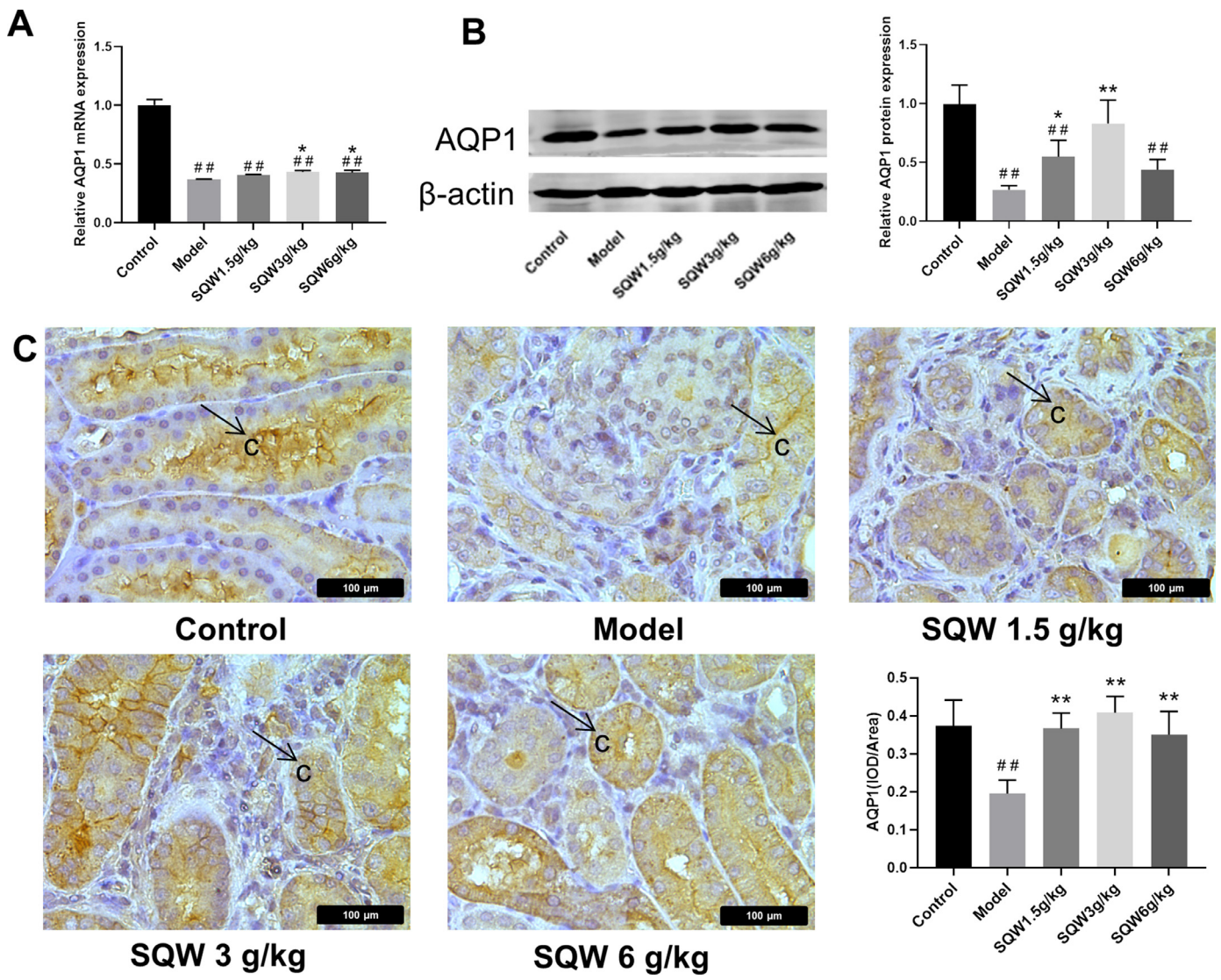

Fig. 4. The effect of SQW on renal AQP1 expression level. (A) The AQP1 mRNA level in the kidney of SD rats was measured by qPCR ($n = 6$). (B) Analysis of AQP1 protein in the kidney of SD rats through Western blot ($n = 6$). (C) Evaluations of AQP1 expression in the kidney of SD rats through immunohistochemistry ($n = 3$). AQP1 is mainly expressed in cytoplasm and cell membrane. (c) Brown granules represent positive AQP1 protein. Small horizontal bars indicate the mean ± S.D. $^{\#}$ $P < 0.05$, $^{\#\#}$ $P < 0.01$ compared with control group; * $P < 0.05$, ** $P < 0.01$ compared with model group. (For interpretation of the references to color in this figure legend, the reader is referred to the web version of this article.)

3.8. Effect of SQW medicated serum on cell migration and lumen forming capacity

The findings of Fig. 5A, B indicated that the lentivirus V2 group could efficiently and stably weaken the AQP1 level in HMEC-1 cells. As shown in Fig. 5C, SQW upregulated AQP1 protein level compared with the control group (NC-10%NRS) and also inhibited downregulated AQP1 protein level with AQP1 knockdown (V2-10%NRS). AQP1 knockdown also inhibited the effect of SQW medicated serum on cell migration and lumen formation (Fig. 6A, B).

4. Discussion

Chronic kidney disease is accompanied by a silent kidney loss due to different disorders like diabetes, high blood pressure, glomerulonephritis, interstitial nephritis, polycystic kidney disease. Indeed CKD is an undecorated public health problem, as large number of the population is affected by it. In this study, the effect of SQW on CKD animal model has been described in this article and we delineated the working principle of SQW in cell lines and animal models.

The animal model provides a meaningful platform to examine the underlying mechanism of therapy against CKD. The adenine-induced rat model is one of the successfully adopted CKD models, manifested in the appearance of the corresponding symptoms, such as lesions of proximal tubules, of some distal tubules. There is a probability to withstand with the CKD to targeted repair of peritubular capillary endothelium and glomeruli (Diwan et al., 2018). Adenine treatment-induced destruction of renal structure and function in rats' renal tissue appeared and hence provided a suitable model to analyze pathological markers- BUN, Scr, and U-TP/24 h, morphological changes of kidney fibrosis with accordance to the conventional CKD syndrome (Chen et al., 2017). Serum BUN, SCr, and U-TP/24 h urine protein are the indicators of renal function, and a significant increase of these proteins in CKD are highly measured. Moreover, with SQW, a reduced serum BUN, SCr, and U-TP urine protein were observed, indicating improved renal function. Hypothalamic-pituitary-adrenal (HPA) axis

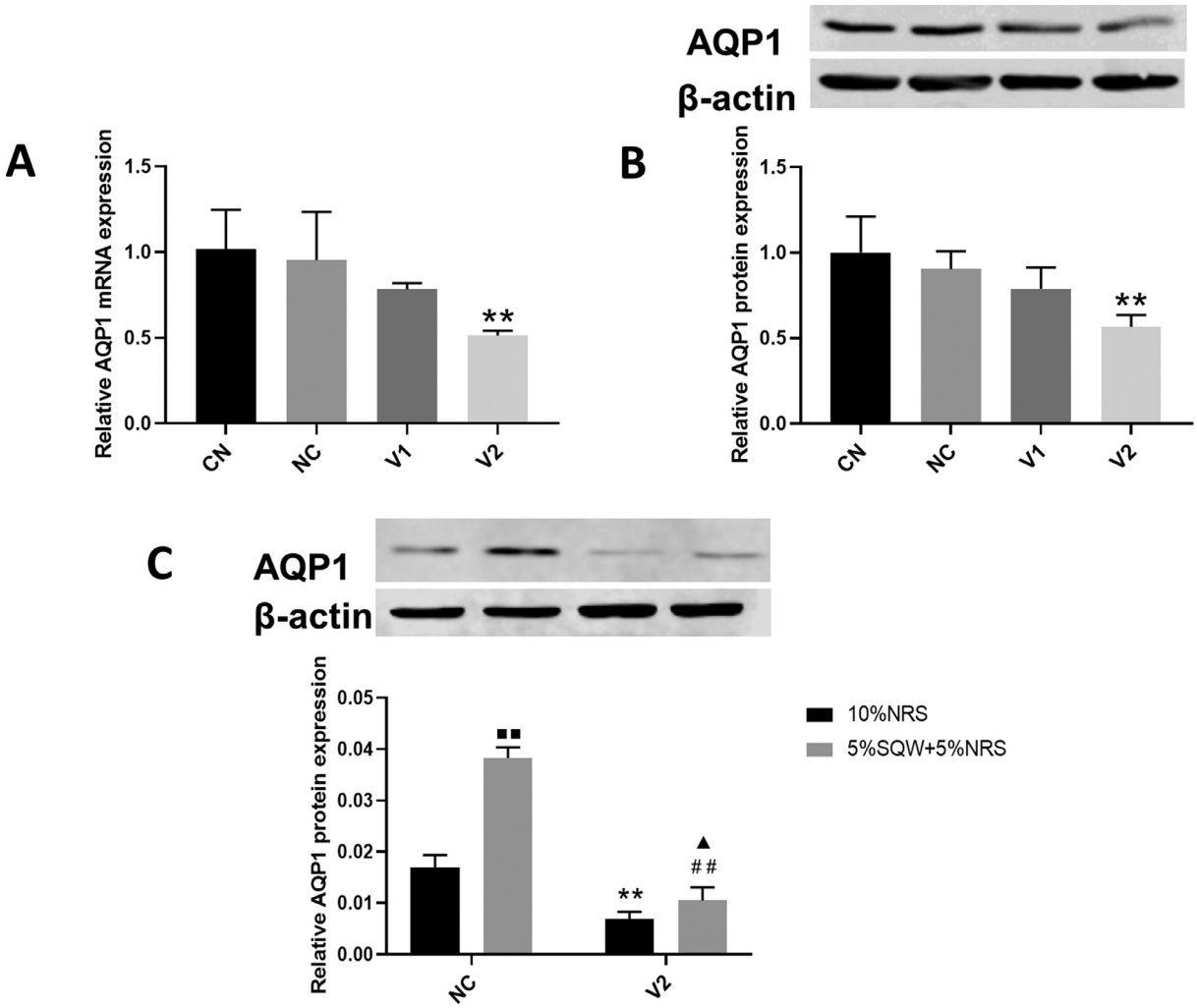

Fig. 5. Effect of AQP1 knockdown on the AQP1 expression in HMEC-1 cells. (A) Effect of different interference targets of AQP1 RNAi lentivirus (V1, V2) and negative control (NC) on mRNA expression of AQP1 in HMEC-1 cells ($n = 4$). mean ± S.D. ** $P < 0.01$ compared with negative control group. (B) Effect of different interference targets of AQP1 RNAi lentivirus (V1, V2) and negative control (NC) on protein expression of AQP1 in HMEC-1 cells ($n = 4$). mean ± S.D. ** $P < 0.01$ compared with negative control group. (C) With lentivirus V2 and SQW (3 g/kg) medicated serum treatment, the protein expression of AQP1 was detected by western blot ($n = 4$). mean ± S.D. $^{■}P < 0.05$, $^{■■}P < 0.01$ compared with NC-10%NRS; $^{\#}P < 0.05$, $^{\#\#}P < 0.01$ compared with V2-10%NRS; $^{**}P < 0.01$ compared with NC-10%NRS; $^{▲}P < 0.05$ compared with NC-5% SQW + 5% NRS. (CN: control group, NC: negative control group, V1: the lentivirus V1 group , V2: the lentivirus V2 group, NRS: Normal rat serum).

markers, including CRH, ACTH, CORT, and 17-OHCS, are associated with end-stage renal disease, which is highly suppressed in CKD patients (Cardoso et al., 2016). The hormonal imbalance was observed in CKD disorder. Adenine administration also caused an increase in these hormonal levels which showed improvement in the presence of SQW.

Consequently, peritubular capillary injury in kidney tissue with adenine is noticed, is usually accompanied by CKD-like symptoms (Kramann et al., 2014). The loss of peritubular capillaries is a common feature of progressive renal disease (Tanaka and Nangaku, 2013), common in both animal models and renal disease patients (Babickova et al., 2017). At this stage, the function of the endothelial cells are compromised (Ligresti et al., 2016). Endothelial cells, serving as the inner lining of the vessel wall, often assemble to form a lumen and consist of many blood vessels that supply and deliver nutrients and oxygen to the body (Watson et al., 2017; Rohlenova et al., 2018). The endothelium cells are the main components of blood vessels, thus playing a nodal role in angiogenesis. Previous evidence showed that VEGF is a key mediator of vascular formation (Carmeliet et al., 1996). Physiological events, including cell proliferation, migration, survival, and vascular permeability during vasculogenesis and angiogenesis, were affected by VEGF signaling by regulating several kinases' activities (Apte et al., 2019). The results of our research indicated that the group related to peritubular injury showed a low level of VEGF expression favoring the earlier findings (Krieter et al., 2010).

Water channel protein-AQP1 maintains the osmotic balance in the renal which is associated with cell migration and angiogenesis (Narvaez-Moreno et al., 2019). Recently adequate evidence supported that inhibition of AQP1 relates to impaired migration, invasion, and tubulogenesis *in vitro* (Tomita et al., 2019; Shu et al., 2019). We have shown AQP1 knockdown inhibited cell migration and tube formation that was enhanced by SQW administration. Moreover, SQW was able to upregulate AQP1 expression in the cells both *in vitro* and *in vivo*. AQP1 was uncovered as an important target for SQW. The silencing of AQP1 diluted the effect of SQW in the *in vitro* conditions was encouraging delineating the molecular pathway for SQW in CKD pathogenesis *in vitro* and *in vivo*. However, future studies would be needed to support our findings in the *in vivo* knockout system fully.

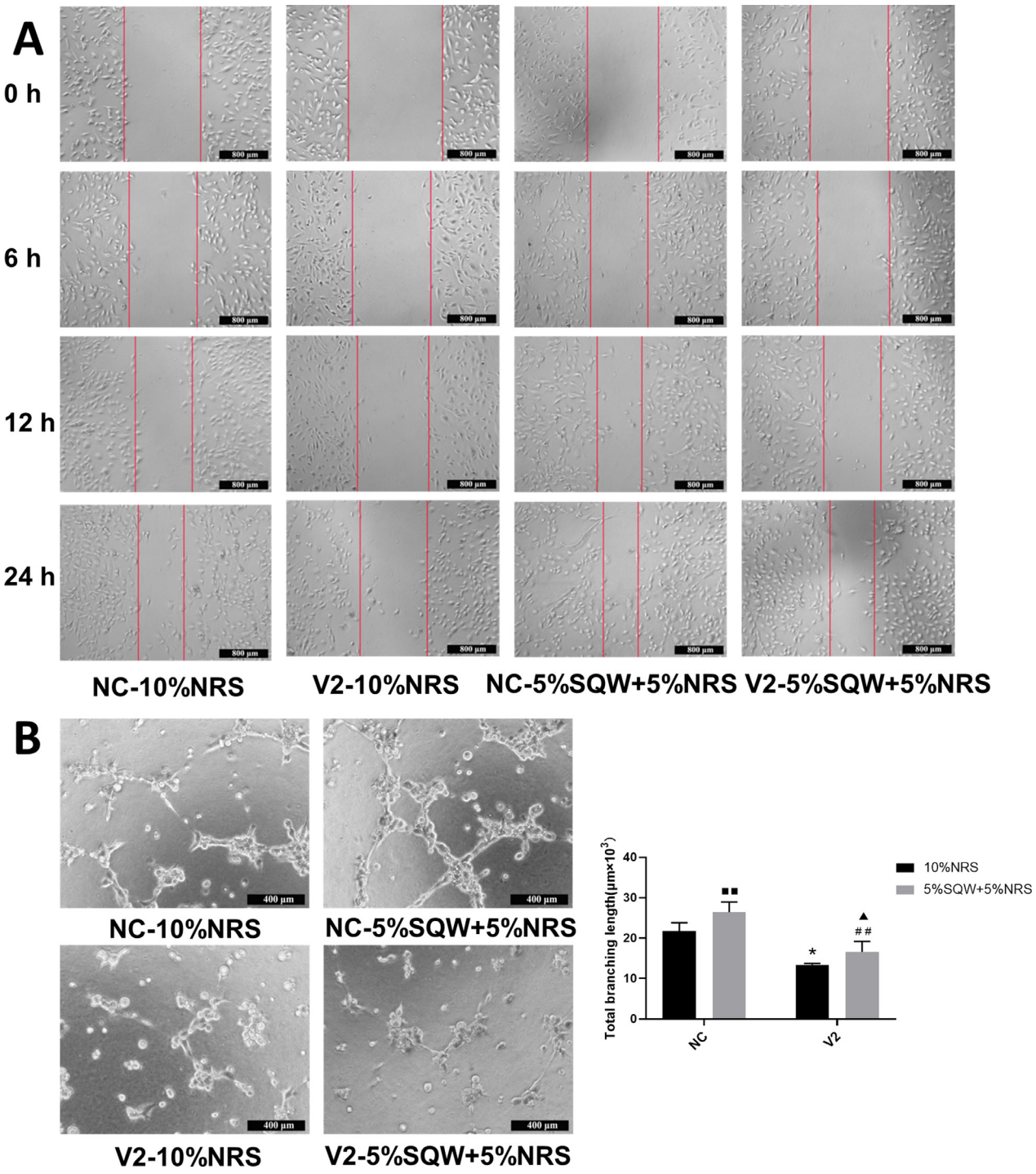

Fig. 6. Effect of SQW on promoting cell migration and tube formation after AQP1 knockdown in HMEC-1 cells. (A) Indice for angioplasty ability-Representative images of cell migration (n = 4). mean ± S.D.■■P < 0.01 compared with NC-10%NRS,**P < 0.01 compared with NC-10%NRS, ▲P < 0.05 compared with V2-10% NRS, # # P < 0.01 compared with NC-5% SQW + 5% NRS. (B) Indice for angioplasty ability-Representative images of tube formation (n = 4). mean ± S.D. ■■P < 0.01 compared with NC-10%NRS,*P < 0.01 compared with NC-10%NRS, ▲P < 0.05 compared with V2-10% NRS, # # P < 0.01 compared with NC-5% SQW + 5% NRS. (NC: negative control group, V2: the lentivirus V2 group , NRS: Normal rat serum, SQW: shenqiwan)

5. Conclusion

Our results led to conclude that SQW restores peritubular capillary injury in adenine-induced CKD rats. SQW also significantly inhibited the inflammatory cytokines including MCP-1 and VCAM-1 levels. Meanwhile, SQW treatment enhanced AQP1 expression in the renal cells and tissues. SQW also facilitated angiogenesis process, which was hampered in the CKD model system. It has been demonstrated that SQW administration attenuated renal vascular injury by boosting the angiogenesis of endothelial cells. The protective effect of SQW on the angiogenesis of endothelial cells provided a novel perspective for the treatment of CKD.

Ethical approval

The animal experiments were approved by the Ethics of Committee of Zhejiang Traditional Chinese Medical University (ZSLL-2017-054).

Data availability

The data used to support the findings of this study are available from the corresponding author upon request.

The processed data required to reproduce these findings cannot be shared at this time as the data also forms part of an ongoing study.

Funding

This work is supported by National Natural Science Foundation of China (Grant No. 8167151544), 2020 Zhejiang University Student Science and Technology Innovation Activity Plan and New Seed Talent Project (No. 2020R410058).

Declaration of Competing Interest

The authors declare that there is no conflict of interest regarding the publication of this paper.

CRediT authorship contribution statement

Yuting Bao: Visualization, Investigation. **Yehui Zhang:** Formal analysis, Writing – original draft. **Yuanxiao Yang:** Supervision. **Xueming Chen:** Investigation. **Luning Lin:** Investigation. **Yunbo Fu:** Investigation. **Liting Ji:** Visualization, Supervision. **Changyu Li:** Visualization, Supervision.

Acknowledgments

We are indebted to the members of our laboratories at the Department of pharmacology, University of Zhejiang Chinese Medical.

Supplementary materials

Supplementary material associated with this article can be found, in the online version, at doi:10.1016/j.ccmp.2021.100010.

ORCID

Changyu Li, https://orcid.org/0000-0001-8656-0428.

References

Apte, R.S., Chen, D.S., Ferrara, N., 2019. VEGF in signaling and disease: beyond discovery and development. Cell 176, 1248–1264. doi:10.1016/j.cell.2019.01.021.

Babickova, J., Klinkhammer, B.M., Buhl, E.M., Djudjaj, S., Hoss, M., Heymann, F., Tacke, F., et al., 2017. Regardless of etiology, progressive renal disease causes ultrastructural and functional alterations of peritubular capillaries. Kidney Int. 91, 70–85. doi:10.1016/j.kint.2016.07.038.

Cardoso, E.M., Arregger, A.L., Budd, D., Zucchini, A.E., Contreras, L.N., 2016. Dynamics of salivary cortisol in chronic kidney disease patients at stages 1 through 4. Clin. Endocrinol. 85, 313–319. doi:10.1111/cen.13023, (Oxf).

Carmeliet, P., Ferreira, V., Breier, G., 1996. Abnormal blood vessel development and lethality in embryos lacking a single VEGF allele. Nature 380, 435–439.

Chen, H., Xu, Y., Yang, Y., Zhou, X., Dai, S., Li, C., 2017. Shenqiwan ameliorates renal fibrosis in rats by inhibiting TGF-β1/smads signaling pathway. Evid. Based Complement. Altern. Med., 7187038 doi:10.1155/2017/7187038, 2017.

Denic, A., Glassock, R.J., Rule, A.D., 2016. Structural and functional changes with the aging kidney. Adv. Chronic Kidney Dis. 23, 19–28. doi:10.1053/j.ackd.2015.08.004.

Diwan, V., Brown, L., Gobe, G.C., 2018. Adenine-induced chronic kidney disease in rats. Nephrology 23, 5–11. doi:10.1111/nep.13180, (Carlton).

Dong, W., Xian, Y., Yuan, W., Huifeng, Z., Tao, W., Zhiqiang, L., Shan, F., et al., 2016. Catalpol stimulates VEGF production via the JAK2/STAT3 pathway to improve angiogenesis in rats' stroke model. J. Ethnopharmacol. 191, 169–179. doi:10.1016/j.jep.2016.06.030.

Eelen, G., de Zeeuw, P., Treps, L., Harjes, U., Wong, B.W., Carmeliet, P., 2018. Endothelial cell metabolism. Physiol. Rev. 98, 3–58. doi:10.1152/physrev.00001.2017.

Kramann, R., Tanaka, M., Humphreys, B.D., 2014. Fluorescence microangiography for quantitative assessment of peritubular capillary changes after AKI in mice. J. Am. Soc. Nephrol. 25, 1924–1931. doi:10.1681/ASN.2013101121.

Krieter, D.H., Fischer, R., Merget, K., Lemke, H.D., Morgenroth, A., Canaud, B., Wanner, C., 2010. Endothelial progenitor cells in patients on extracorporeal maintenance dialysis therapy. Nephrol. Dial. Transplant. 25, 4023–4031. doi:10.1093/ndt/gfq552.

Lemley, K.V., 2016. Glomerular pathology and the progression of chronic kidney disease. Am. J. Physiol. Ren. Physiol. 310, F1385–F1388. doi:10.1152/ajprenal.00099.2016.

Li, L., Kang, H., Zhang, Q., D'Agati, V.D., Al-Awqati, Q., Lin, F., 2019. $FoxO_3$ activation in hypoxic tubules prevents chronic kidney disease. J. Clin. Investig. 129, 2374–2389. doi:10.1172/jci122256.

Ligresti, G., Nagao, R.J., Xue, J., Choi, Y.J., Xu, J., Ren, S., Aburatani, T., et al., 2016. A novel three-dimensional human peritubular microvascular system. J. Am. Soc. Nephrol. 27, 2370–2381. doi:10.1681/ASN.2015070747.

Lin, S.L., Chang, F.C., Schrimpf, C., Chen, Y.T., Wu, C.F., Wu, V.C., Chiang, W.C., et al., 2011. Targeting endothelium-pericyte cross talk by inhibiting VEGF receptor signaling attenuates kidney microvascular rarefaction and fibrosis. Am. J. Pathol. 178, 911–923. doi:10.1016/j.ajpath.2010.10.012.

Munoz-Felix, J.M., Oujo, B., Lopez-Novoa, J.M., 2014. The role of endoglin in kidney fibrosis. Expert Rev. Mol. Med. 16, e18. doi:10.1017/erm.2014.20.

Narvaez-Moreno, B., Sendin-Martin, M., Jimenez-Thomas, G., Sanchez-Silva, R., Suarez-Luna, N., Echevarria, M., Bernabeu-Wittel, J., 2019. Expression patterns of Aquaporin 1 in vascular tumours. Eur. J. Dermatol. 29, 366–370. doi:10.1684/ejd.2019.3602.

Palethorpe, H.M., Tomita, Y., Smith, E., Pei, J.V., Townsend, A.R., Price, T.J., Young, J.P., Yool, A.J., Hardingham, J.E., 2018. The Aquaporin 1 inhibitor bacopaside II reduces endothelial cell migration and tubulogenesis and induces apoptosis. Int. J. Mol. Sci. 19. doi:10.3390/ijms19030653.

Qiu, C., Huang, S., Park, J., Park, Y., Ko, Y.A., Seasock, M.J., Bryer, J.S., et al., 2018. Renal compartment-specific genetic variation analyses identify new pathways in chronic kidney disease. Nat. Med. 24, 1721–1731. doi:10.1038/s41591-018-0194-4.

Rabelink, T.J., Wijewickrama, D.C., de Koning, E.J., 2007. Peritubular endothelium: the achilles heel of the kidney? Kidney Int. 72, 926–930. doi:10.1038/sj.ki.5002414.

Roediger, B., Lee, Q., Tikoo, S., Cobbin, J.C.A., Henderson, J.M., Jormakka, M., O'Rourke, M.B., et al., 2018. An atypical parvovirus drives chronic tubulointerstitial nephropathy and kidney fibrosis. Cell 175, 530–543. doi:10.1016/j.cell.2018.08.013, e24.

Rohlenova, K., Veys, K., Miranda-Santos, I., De Bock, K., Carmeliet, P., 2018. Endothelial cell metabolism in health and disease. Trends Cell Biol. 28, 224–236. doi:10.1016/j.tcb.2017.10.010.

Romagnani, P., Remuzzi, G., Glassock, R., Levin, A., Jager, K.J., Tonelli, M., Massy, Z., Wanner, C., Anders, H.J., 2017. Chronic kidney disease. Nat. Rev. Dis. Primers 3, 17088. doi:10.1038/nrdp.2017.88.

Shu, C., Shu, Y., Gao, Y., Chi, H., Han, J., 2019. Inhibitory effect of AQP1 silencing on adhesion and angiogenesis in ectopic endometrial cells of mice with endometriosis through activating the Wnt signaling pathway. Cell Cycle 18, 2026–2039. doi:10.1080/15384101.2019.1637202.

Tanaka, T., Nangaku, M., 2013. Angiogenesis and Hypoxia in the Kidney. Nat. Rev. Nephrol. 9, 211–222. doi:10.1038/nrneph.2013.35.

Tomita, Y., Palethorpe, H.M., Smith, E., Nakhjavani, M., Townsend, A.R., Price, T.J., Yool, A.J., Hardingham, J.E., 2019. Bumetanide-derived Aquaporin 1 inhibitors, AqB013 and AqB050 inhibit tube formation of endothelial cells through induction of apoptosis and impaired migration *in vitro*. Int. J. Mol. Sci. 20. doi:10.3390/ijms20081818.

van Koppen, A., Joles, J.A., Bongartz, L.G., van den Brandt, J., Reichardt, H.M., Goldschmeding, R., Nguyen, T.Q., Verhaar, M.C., 2012. Healthy bone marrow cells reduce progression of kidney failure better than CKD bone marrow cells in rats with established chronic kidney disease. Cell Transplant. 21, 2299–2312. doi:10.3727/096368912X636795.

Venkatachalam, M.A., Weinberg, J.M., Kriz, W., Bidani, A.K., 2015. Failed tubule recovery, AKI-CKD transition, and kidney disease progression. J. Am. Soc. Nephrol. 26, 1765–1776. doi:10.1681/ASN.2015010006.

Verkman, A.S., Anderson, M.O., Papadopoulos, M.C., 2014. Aquaporins: important but elusive drug targets. Nat. Rev. Drug Discov. 13, 259–277. doi:10.1038/nrd4226.

Wang, X., Zhang, A., Zhou, X., Liu, Q., Nan, Y., Guan, Y., Kong, L., et al., 2016. An integrated chinmedomics strategy for discovery of effective constituents from traditional herbal medicine. Sci. Rep. 6, 18997. doi:10.1038/srep18997.

Watson, E.C., Grant, Z.L., Coultas, L., 2017. Endothelial cell apoptosis in angiogenesis and vessel regression. Cell Mol. Life Sci. 74, 4387–4403. doi:10.1007/s00018-017-2577-y.

Wuttke, M., Li, Y., Li, M., Sieber, K.B., Feitosa, M.F., Gorski, M., Tin, A., et al., 2019. A catalog of genetic loci associated with kidney function from analyses of a million individuals. Nat. Genet. 51, 957–972. doi:10.1038/s41588-019-0407-x.

Yen, M.L., Su, J.L., Chien, C.L., Tseng, K.W., Yang, C.Y., Chen, W.F., Chang, C.C., Kuo, M.L., 2005. Diosgenin induces hypoxia-inducible factor-1 activation and angiogenesis through estrogen receptor-related phosphatidylinositol 3-kinase/AKT and P38 mitogen-activated protein kinase pathways in osteoblasts. Mol. Pharmacol. 68, 1061–1073. doi:10.1124/mol.104.010082.

Zhang, J.Y., Hong, C.L., Chen, H.S., Zhou, X.J., Zhang, Y.J., Efferth, T., Yang, Y.X., Li, C.Y., 2019. Target identification of active constituents of Shen Qi Wan to treat kidney yang deficiency using computational target fishing and network pharmacology. Front. Pharmacol. 10, 650. doi:10.3389/fphar.2019.00650.

Zheng, A.X., 2018. Determination of morroniside, loganin and paeonol in Guifu Dihuang pills (concentrated pills) by HPLC. Strait Pharm. J. 30, 66–68. doi:10.3969/j.issn.1006-3765.2018.10.022.

Zhou, F., Qian, Z., Huang, L., 2019. Low-dose mifepristone increased angiogenesis in a manner involving AQP1. Arch. Gynecol. Obstet. 299, 579–584. doi:10.1007/s00404-018-4989-9.